The tetragonal $\leftrightarrow$ phase transition in mixed perovskite Ba$_{1-x}$Ca$_x$TiO$_3$ single crystals: EPR evidence of impurity-induced dynamic effects

The tetragonal ↔ cubic phase transition in mixed perovskite $Ba_{1-x}Ca_xTiO_3$ single crystals: EPR evidence of impurity-induced dynamic effects

Y Babu†, M D Sastry†, B A Dasannacharya‡, S Balakumar§, R Ilangovan§, P Ramasamy§ and M D Aggarwal‖

† Radiochemistry Division, Bhabha Atomic Research Centre, Trombay, Bombay 400085, India
‡ Solid State and Spectroscopy Group, Bhabha Atomic Research Centre, Trombay, Bombay 400085, India
§ Crystal Growth Centre, Anna University, Madras 600 025, India
‖ Department of Physics, Alabama A and M University, Normal, Alabama 35762, USA

Abstract. By using EPR of Fe^{3+} probe ions in $Ba_{1-x}Ca_xTiO_3$ ($x = 0$ and 0.05), clear evidence has been obtained for the existence of dynamic fluctuation between cubic and tetragonal phases in the vicinity of the phase transition temperature. This was manifested as a total absence of the EPR of Fe^{3+} in the temperature range 112–160 °C for $x = 0.05$, clearly showing that there is a time-dependent interaction serving as an additional and more effective pathway of spin relaxation. The time scale of the fluctuation is estimated to be 6×10^{-11} s.

1. Introduction

1.1. Mixed perovskites and their phase transitions

In view of the multitude of applications of $BaTiO_3$ in a variety of devices, it has been and continues to be of interest for investigations using a number of techniques. It undergoes a transition from the ferroelectric tetragonal phase to the paraelectric cubic phase at around 130 °C. Properties of $BaTiO_3$ mixed with homovalent ions like Ca^{2+} and Sr^{2+} have been investigated using neutron and x-ray scattering in addition to the more common dielectric measurements at low frequencies [1–13]. The interest in the mixed compounds arises due to the possibility of 'tailoring' them for various devices. The effects of homovalent and heterovalent substituents on the phase transitions, particularly the ferroelectric → paraelectric transition, have been investigated in $BaTiO_3$ and the results have been reviewed by Pande *et al* [7] and Godefroy *et al* [10]. Darlington and Cernik [11, 12] reported the results of x-ray scattering experiments on the effects of homovalent and heterovalent impurities on the ferroelectric phase transition in $BaTiO_3$. It has been reported [7, 8] on the basis of dielectric studies both on ceramic and on single-crystalline samples that the tetragonal ↔ cubic (T ↔ C) phase transition shows a 'diffuse' character on Ca substitution. However, neutron-scattering studies [9] on ceramic $Ba_{1-x}Ca_xTiO_3$ (BCT) showed a sharp drop in tetragonality (c/a) and the transformation of the sample to cubic phase at temperatures higher than that reported for $BaTiO_3$. This and the hysteresis present showed that the structural transition continued to be of first order even though the

dielectric constant exhibited a broad continuous peak. The analysis of the neutron data further gave evidence for the possible coexistence of cubic and tetragonal phases several degrees below the tetragonal-to-cubic transition. Sastry *et al* [13] recently performed single-crystal neutron diffraction studies on BCT (5% Ca) at several temperatures and found anomalous variations in the Debye–Waller factor associated with the Ti atom, well before the $T \rightarrow C$ transition. Their study also suggests the possibility of large fluctuations in the position of Ti at around $120\,°C$ in single crystals with 5% Ca. Such phenomena should be amenable to direct detection and investigation using electron paramagnetic resonance (EPR) spectroscopy [14, 15], especially with regard to the symmetry of the TiO_6 octahedron when the Fe^{3+} probe ion occupies the Ti^{4+} site. This paper reports such investigations, using Fe^{3+} as probe ion, on flux-grown $Ba_{1-x}Ca_xTiO_3$ single crystals with $x = 0$ and 0.05, and on seed-grown pure $BaTiO_3$.

1.2. The relevance of EPR of Fe^{3+} to study the fluctuations at the $T \leftrightarrow C$ transition

EPR of Fe^{3+} in $BaTiO_3$ and $SrTiO_3$ has been used extensively to provide considerable insight into the nature of phase transitions in these systems [14–22]. The $[FeO_6]^{9-}$ unit acts as the probe complex and can be used to monitor the changes that occur in the crystal. The present work is mainly directed towards investigating the possible fluctuations in the vicinity of the tetragonal $\leftrightarrow$ cubic phase transition caused by calcium doping. The interaction energy of the probe in a tetragonal field is given [23] by the Hamiltonian

$$H = D[3S_z^2 - S(S + 1)] + \tfrac{1}{6}a[S_x^4 + S_y^4 + S_z^4 - \tfrac{1}{5}S(S + 1)(3S^2 + 3S - 1)]$$
$$+ (1/180)F[35S_z^2 - 30S(S + 1)S_z^2 + 25S_z^2 - 6S(S + 1) + 3S^2(S + 1)^2] \quad (1)$$

where D and F are the second- and fourth-order parameters in axial crystal fields. In the case of a tetragonal field the $J = \tfrac{5}{2}$ state splits into three Kramers doublets. The energy levels of these states are given [23] by

$$E_1 = -\tfrac{1}{2}a + \tfrac{2}{3}F + \tfrac{4}{3}D + \{[a + \tfrac{2}{3}F + 2D]^2 + \tfrac{5}{4}a^2\}^{1/2}$$
$$E_2 = -\tfrac{1}{2}a + \tfrac{2}{3}F + \tfrac{4}{3}D - \{[a + \tfrac{2}{3}F + 2D]^2 + \tfrac{5}{4}a^2\}^{1/2}$$
$$E_3 = a + \tfrac{2}{3}F - \tfrac{8}{3}D. \quad (2)$$

In a cubic field, $D = F = 0$ and, from the expression given above, the zero-field splitting between the quartet and the doublet is seen to be $3a$. In a tetragonal field, normally $D \gg a$, F and the splittings between the doublets are approximately $2D$ and $4D$, making the total zero-field splitting equal to $6D$. At the tetragonal $\rightarrow$ cubic transition $D \rightarrow 0$ and hence 'D' can be used as the 'order parameter'. More interestingly, if the Fe^{3+} probe is subjected to a fluctuating crystal field, it can bring about a time-dependence in D, which in turn can contribute to relaxation. This aspect is used in the present work in identifying temporal fluctuation of the site symmetry at the Fe^{3+} (Ti^{4+}) site on doping with Ca.

2. Experimental

Seed-grown single crystals of $BaTiO_3$ were grown at Alabama A & M University, Normal, Alabama, using the pulling technique. Flux-grown single crystals of $Ba_{1-x}Ca_xTiO_3$ with $x = 0$ and 0.05 were grown using Remeika's method at the Crystal Growth Centre, Anna University, Madras. The crystals with $x = 0.05$ were grown by adding 20 at% Ca to the melt. The actual concentration of Ca in the crystals was determined by an emission spectrometric method. In this method, a known amount of the sample was diluted with

spectroscopically pure graphite and was excited in a *DC* arc together with graphite standards containing known concentrations of Ca. The emission spectra of the samples and standards were recorded on a Jarrell–Ash direct reading spectrometer. From the Ca emission intensities due to the sample and standards, the concentration of Ca in the sample was determined. The analysis of the crystals has shown the presence of only 5 at% of Ca and hence x is taken to be 0.05. This crystal containing 5% calcium is referred to as barium calcium titanate (BCT) in this paper, whereas $x = 0$ (no calcium) is referred to as barium titanate (BT). The EPR spectra were recorded on a Bruker ESP-300 spectrometer operating in the X band. Temperature variation in the range 30-200 °C was performed using a Varian variable-temperature accessory. Orientation of single crystals in the magnetic field was accomplished by using a goniometer.

3. Results and discussion

3.1. Experimental results

It is well-established that Fe^{3+} occurs at very low concentrations in $BaTiO_3$ and its EPR has been reported by various workers [14–22]. Both nominally pure (seed-grown and flux-grown) and Ca-substituted single crystals showed the EPR spectra due to Fe^{3+} ions in the present work. The temperature-dependence of the Fe^{3+} spectrum in the 30–200 °C range was used to monitor the effects of Ca substitution on the phase transitions in $BaTiO_3$ single crystals. In view of its very low concentration (50–100 ppm) Fe^{3+} does not affect the bulk properties and it is a convenient probe to investigate the microscopic changes that take place during the phase transition.

In the seed-grown crystal ($x = 0$), sharp and intense EPR lines were obtained for Fe^{3+}. These spectra were similar to those reported in the literature. The five fine-structure transitions could be identified for H parallel to a or b. The axial field parameter given in equations (1) and (2), related to the separation between fine-structure transitions, could be followed across the phase transition in this crystal. The spectra showed strong temperature-dependences and the EPR spectra obtained at different temperatures from a pure seed-grown crystal are shown in figure 1. It may be noted that the cubic spectrum appeared just about 1 °C above the disappearance temperature of the tetragonal spectrum. The spin Hamiltonian constants obtained by us are given in table 1, together with those reported by earlier workers. The agreement is satisfactory.

Table 1. Spin Hamiltonian constants for the EPR spectrum of Fe^{3+} at room temperature in BT and BCT.

Crystal system	$g_\parallel$	$g_\perp$	D (cm^{-1})	a (cm^{-1})	Reference
BT	2.0036	2.0036	0.0929	0.0091	[19]
BT	2.003 ± 0.001	2.003 ± 0.001	0.0991	0.0084	This work
BCT	2.003	2.003	0.0945		This work

In view of the significant increase in line width on Ca substitution, a for BCT could not be determined.

In BCT the EPR lines of Fe^{3+} were broader and less intense than that observed in a seed-grown crystal of BT. Figures 2(*a*)–(*c*) show the Fe^{3+} EPR spectra obtained at room temperature (RT) in the single crystal of BCT with magnetic field parallel to the *c* axis, to
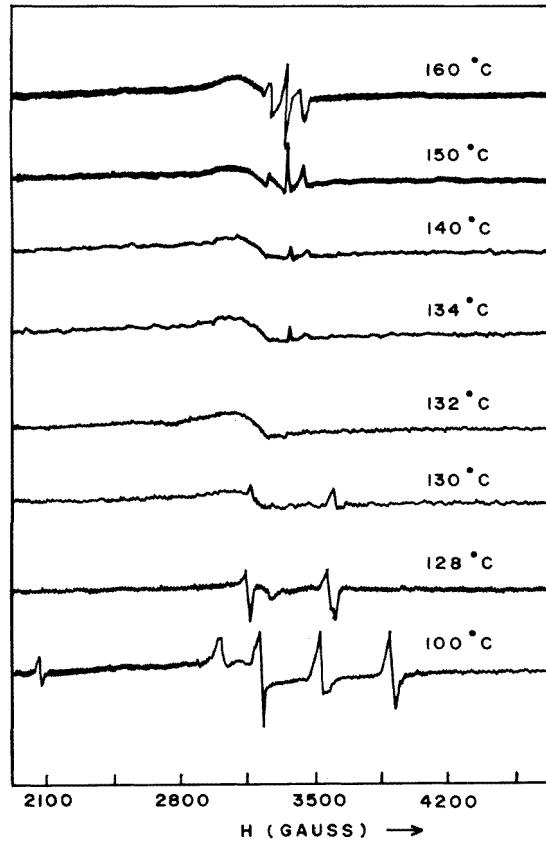
Figure 1. The EPR spectrum of Fe^{3+} in seed-grown $BaTiO_3$ at different temperatures with the magnetic field making an angle of about $37°$ to the c axis in the c–$a(b)$ plane. It can be seen that the tetragonal spectrum disappeared at $132\,°C$ and the cubic spectrum appeared at around $134\,°C$.

the a or b axis and in the a–b plane at an angle of about $40°$ to the a or b axis respectively. The angular variation of the spectrum in the c–a plane of BCT is shown in figure 3. The lowest and highest field lines, $\pm\frac{3}{2} \leftrightarrow \pm\frac{5}{2}$ transitions, could not be followed and hence are not given. The lines broadened significantly with Ca doping. The spectra obtained with H parallel to a or b in flux-grown crystals with $x = 0$ and 0.05 are shown in figure 4. The spin Hamiltonian parameters g and D obtained for BCT are included in table 1. The observation of a weak c-orientation spectrum (especially the $\pm\frac{1}{2} \leftrightarrow \mp\frac{1}{2}$ transition) for H perpendicular to c suggests that the crystals were not entirely monodomain in nature and that a small fraction ($< 5\%$) of $90°$ domains could be present. The spectra from these domains were more clearly seen along the crystallographic axes and broadened at other angles. Therefore, in addition to the predominant spectrum, two other spectra related to the main one would also coexist. The angular variation of one of them is a mirror reflection of the angular variation shown in figure 3 (full curves). The other one is the angular variation observable in the a–b plane. This is also included in figure 3 for completeness (broken curves). It should, however, be stressed that the lines from less dominant domains were not seen clearly away from the principal axes. From the angular variation it is seen that the
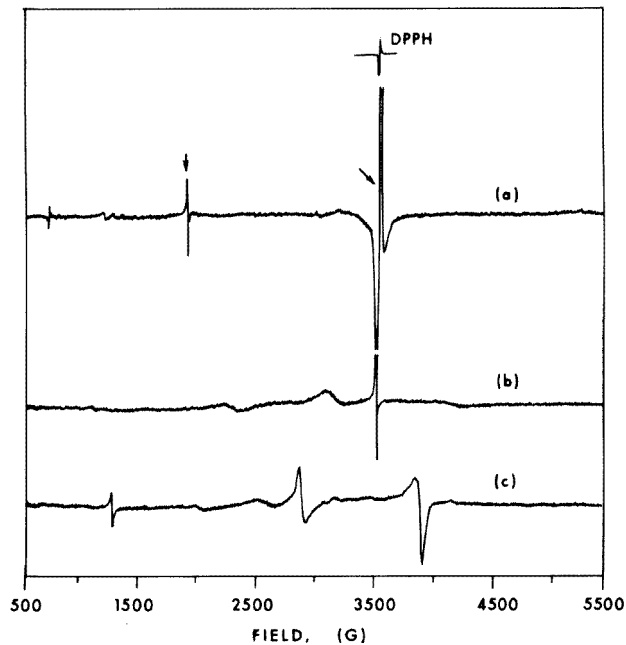
Figure 2. The EPR spectrum of Fe^{3+} in flux-grown $BaCaTiO_3$. (*a*) H parallel to the c axis. The lines marked by arrows are the fine-structure transitions for this orientation. The third is a broader one close to 5500 G. These are shown to highlight the observation of the $\frac{1}{2} \leftrightarrow -\frac{1}{2}$ line of the c spectrum for H perpendicular to c. (*b*) H perpendicular to the c axis. The appearance of a line at $g = 2$ is symptomatic of 90° domains. (*c*) H making an angle of about 40° to the a axis in the a–b plane.

$\frac{1}{2} \leftrightarrow -\frac{1}{2}$ a–b plane, $-\frac{1}{2} \leftrightarrow -\frac{3}{2}$ a–c plane and $\frac{3}{2} \leftrightarrow \frac{1}{2}$ a–b plane transitions occur at nearly the same resonance field for $\theta \approx 37°$. Similarly, the $\frac{1}{2} \leftrightarrow -\frac{1}{2}$ a–b plane and $\frac{3}{2} \leftrightarrow \frac{1}{2}$ a–c plane transitions occur at nearly the same field for this angle. In the temperature-variation experiments, we oriented the crystal with H nearly at 45° to the c axis, and then adjusted the orientation slightly such that the intense lines occurred at around 4200 and 3100 G, leaving the $g = 2$ region completely free of EPR signals in the tetragonal phase. This angle may be taken as $37 \pm 3°$ to the c axis. In the cubic phase the intense line ($\frac{1}{2} \leftrightarrow -\frac{1}{2}$) appears at around 3500 G. It is a very convenient orientation from which to monitor the evolution of the cubic phase from the tetragonal phase with increasing temperature, for the intense lines in the respective phases occur at distinctly different positions even for a multidomain crystal.

Studies of the temperature-dependence of the EPR spectra in the range 30–200 °C, shown in figure 5, revealed some interesting aspects of the tetragonal ↔ cubic transition in the mixed crystal system. When the crystal with $x = 0.05$ was heated the EPR spectrum started to show changes from 105 °C, with the 'tetragonal' line increasingly broadened and distorted. The tetragonal spectrum disappeared at around 112 °C. However, a clear cubic spectrum appeared only above 160 °C. A weak signal at around $g \approx 2$ was seen above 130 °C, which was temperature-independent up to 160 °C. A similar signal was observed from $x = 0$ flux-grown crystals and, therefore, we believe that this arises due to a small unevenness in the Ca distribution. For flux-grown $x = 0$ crystals the temperature window in which EPR signals disappeared was reduced to about 10 °C, but this was a little uncertain
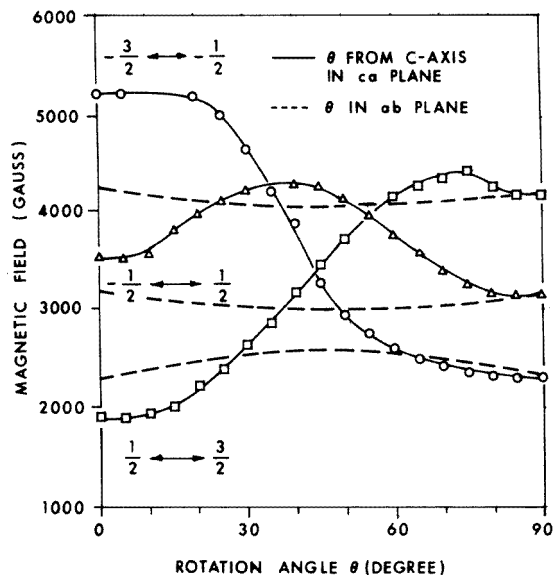
Figure 3. The angular variation of the EPR spectrum of Fe^{3+} in BCT in the *c–a* plane. Only the central three fine-structure transitions are shown. The outermost ones, $\pm\frac{3}{2} \leftrightarrow \pm\frac{5}{2}$ transitions, could not be followed throughout due to the large line width and poor intensity. The angular variation in the *a–b* plane (corresponding to a 90° domain) is also shown using broken curves.

due to the poor intensity of the spectrum in the transition region. For seed-grown $x = 0$ crystals, the temperature window in which the EPR spectra of either phase completely disappeared is very narrow (1–2 °C).

Figure 6 shows the temperature-independence of the axial parameter for BT and BCT. It can be seen that, in the case of BT, it exhibited almost a linear decrease with increasing temperature in the tetragonal phase followed by a sharp fall close to T_c. In comparison, for BCT crystals, the '*D*' parameter was almost temperature-independent.

3.2. Discussion

The temperature-dependence of the *D* parameter in the close vicinity of T_c in BT (figure 6) is in general agreement with results of similar studies reported earlier. The problem of phase transitions in perovskite oxides has been addressed by a number of workers earlier, the most prominent among them being Müller [14]. The temperature-dependence of *D* has been correlated to the temperature-dependence of spontaneous polarization arising from disorder in the Ti position between regular and off-centred positions. Müller and co-workers identified a cross over from displacive to order–disorder behaviour close to T_c. However, in BCT, similar insight has not been possible in view of the complete disappearance of the spectrum. It may be interesting to remember that Müller's work demonstrated that no EPR spectra of Mn^{4+} could be observed in the orthorhombic, tetragonal or cubic phase of BT along the $\langle 111 \rangle$ direction. From this it was inferred that Mn^{4+} and Ti^{4+} move between equivalent $\langle 111 \rangle$ directions with frequency 0.9×10^{10} s^{-1}. Therefore, the disappearance of the EPR spectrum in the close vicinity of T_c in the present studies in BCT deserves special attention.
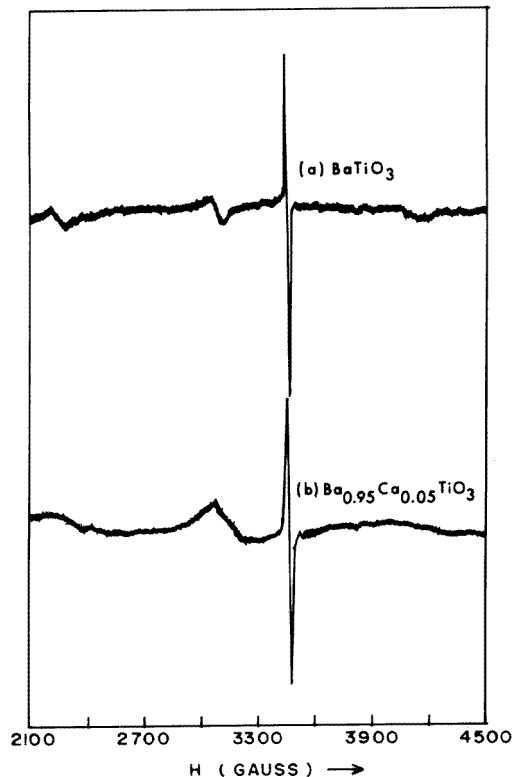
Figure 4. The EPR spectrum of Fe^{3+}: (*a*) in flux-grown BT and (*b*) in flux-grown $Ba_{0.95}Ca_{0.05}TiO_3$. The field orientation in both cases is parallel to $a(b)$. Significant broadening of lines with Ca doping may be observed. The sharp line corresponds to the c spectrum due to $90°$ domains.

The important finding of the present work may, therefore, be stated as follows. During the tetragonal $\leftrightarrow$ cubic phase transition there is a temperature window of about $45\,°C$ in $x = 0.05$ samples, within which the EPR spectrum was absent. This window shrank to $10\,°C$ for flux-grown $x = 0$ samples, and almost disappeared in seed-grown crystals of $BaTiO_3$. Seed-grown crystals are expected to be purer and this was obvious from the quality of the EPR spectrum. Therefore, it is concluded that the temperature window close to T_c in which neither the cubic nor the tetragonal spectrum appears is large in Ca-doped samples and almost vanishes in the case of pure $BaTiO_3$ crystals.

The probe ion Fe^{3+} has a half-filled electronic configuration, $3d^5$ with $^6S_{5/2}$ ground state. For S state ions, the crystal field interaction does not exist in the first order. The crystal field interaction given in the Hamiltonian above (equation (1)) arises due to higher order admixtures of non-S states into the ground state. These interactions split the sixfold degenerate state into three doublets with a maximum separation of $\approx 6D$, as can be seen from equation (2). In view of the predominant S character of the ground state, the spin–lattice relaxation times are sufficiently long, facilitating the observation of EPR over a very wide temperature range. Normally, the spin–lattice relaxation occurs through spin–phonon interactions involving direct, Raman and Orbach processes [23]. These processes have
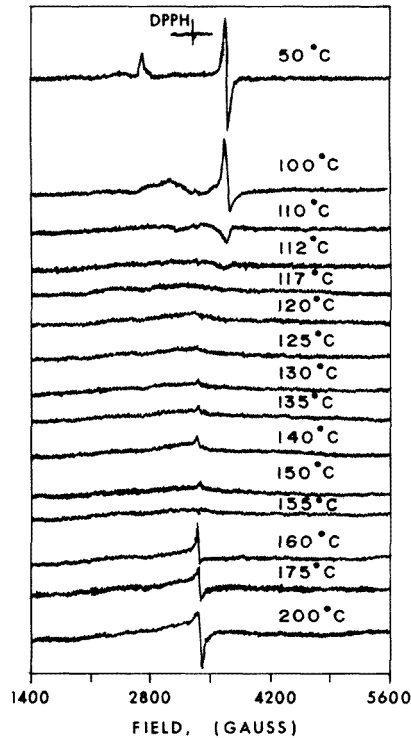
Figure 5. The temperature-dependence of the Fe^{3+} spectrum in BCT across the tetragonal $\leftrightarrow$ cubic transition. The disappearance of EPR signals in the 112–160 °C region may be seen. This may be compared with figure 1, in which the temperature interval within which this happens is only 1–2 °C wide.

well-known temperature-dependences and operate in different temperature ranges. When the 'spin' experiences a fluctuating crystal field it creates a time-dependent interaction with the lattice and if it has spectral density at the resonance frequency, this would add to a new pathway of faster spin–lattice relaxation. If T_1 decreases to $\leqslant 10^{-10}$ s, the disappearance of the EPR spectrum would result.

The observation neither of the cubic spectrum nor of the tetragonal spectrum in the Ca-doped crystal sample in the temperature range 112–160 °C suggests that a dynamic mechanism for fast spin–lattice relaxation may be operating in this temperature range. Because this happened in the vicinity of the phase transition, the most probable reason appears to be a dynamical coexistence of local cubic and tetragonal phases, as seen by EPR through the TiO_6 unit; that is, the system is undergoing temporal fluctuations between these two phases at microscopic level. In the tetragonal phase of pure $BaTiO_3$, the interaction energy (zero-field splitting) of the paramagnetic probe Fe^{3+} was reported to be ≈ 0.588 cm^{-1} whereas in the cubic phase it was 0.03 cm^{-1} [19]. From the D values obtained in BCT (see table 1), it is seen to be marginally smaller than that in BT and it is concluded that there is no substantial change in the zero-field splitting (ZFS) of Fe^{3+} at room temperature with calcium doping. Whereas the ZFS has shown a strong temperature-dependence in $x = 0$ crystals, it was nearly temperature-independent in the tetragonal phase of BCT. Hence, in
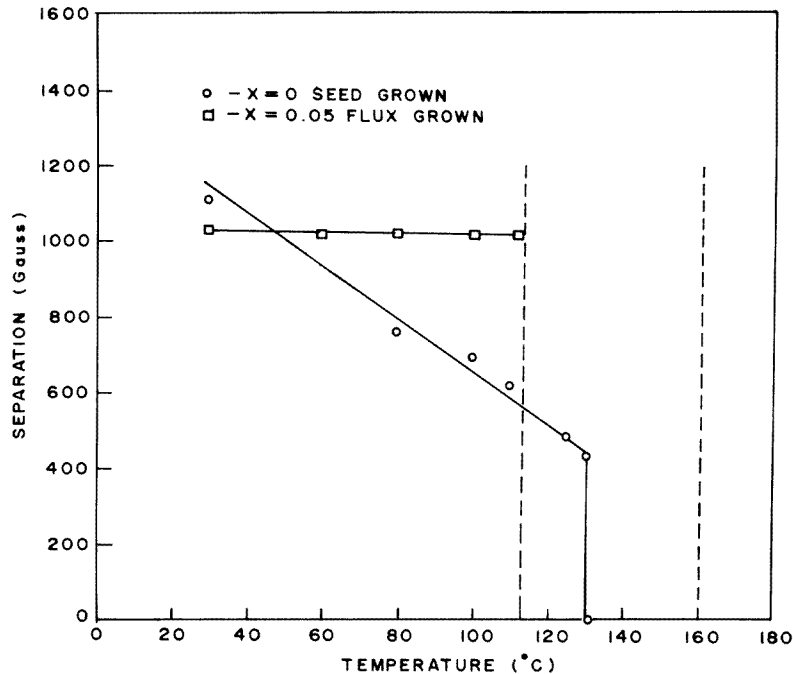
Figure 6. The temperature dependence of the fine-structure parameter D for BT and BCT. It may be noted that D for BCT does not show much temperature-dependence, in contrast to the strong temperature-dependence for D of BT. In the temperature region bounded by the dotted lines, the EPR spectrum disappears in BCT.

BCT, if the time scale of the fluctuation is longer than the inverse of the ZFS in frequency units (6×10^{-11} s), then static coexistence of the two phases should be seen. If the time scale is much smaller than this characteristic value, an averaged spectrum should be seen. However, if the time scale of fluctuation is of the order of 6×10^{-11} s, the spectrum should disappear because this fluctuation acts as a preferential pathway for spin–lattice relaxation. The present experimental results are consistent with only the last possibility. The time scale of fluctuation is thus estimated to be $\approx 6 \times 10^{-11}$ s, which is less than the time scale of EPR and hence the spectrum disappears. This fluctuation in Ti position should result in certain anomalies in the vibrational behaviour of the Ti sub-lattice in the 112–160 °C temperature range. The anomaly observed in the Debye–Waller factor for Ti atoms in neutron scattering [13] is consistent with these EPR results. Rekha Rao *et al* [24] found that the intensity of the Raman active modes in the tetragonal phase vanished above 105 °C. It may be recalled that changes in the EPR spectrum are also detected at around this temperature. Furthermore, they observed quasi-elastic light scattering up to 145 °C. The above features are attributed to the existence of large dynamic disorder associated with Ti and O1 atoms along the c axis in the temperature range 100–145 °C. In view of the evidence obtained using these three different techniques in our laboratory, we conclude that homovalent doping of barium titanate with calcium results in dynamic fluctuation in the position of Ti over a very wide temperature. A pure cubic phase is stabilized at a much higher temperature ($\geqslant$ 160 °C) compared with undoped $BaTiO_3$.

4. Summary

EPR studies performed on flux-grown single crystals of $Ba_{0.95}Ca_{0.05}TiO_3$ have provided clear evidence for the dynamic fluctuation of the Ti position in the 112–160 °C temperature range, with a correlation time estimated to be of the order of 6×10^{-11} s.

Acknowledgments

References

[1] Hennings D and Schreinemacher H 1977 *Mater. Res. Bull.* **12** 1221
[2] Lin J N and Wu T B 1991 *J. Appl. Phys.* **68** 985
[3] Yoon K H, Kim J H, Jo K H, Song H I, Yoon S O and Kim C S 1988 *J. Mater. Sci.* **23** 61
[4] Mitsui T and Westphal W B 1961 *Phys. Rev.* **124** 1354
[5] Tsai-Fa Lin, Chen-Ti Hu and Nan Lin I 1990 *J. Appl. Phys.* **67** 1042
[6] Zhuang Z Q, Harmer M P, Smyth D M and Newnham R E 1987 *Mater. Res. Bull.* **22** 1329
[7] Dhananjai Pandey, Tiwari V S, Singh T B, Lakshman Pandey, Om Parkash and Ramachandra Rao P 1987
        Phase Transitions **9** 11
[8] Balakumer S, Ilangovan R, Balasundaram N and Subramanian C 1992 *Solid State Physics (India)* C **35** 383
[9] Tiwari V S, Pandey D, Krishna P S R, Chakravarthi R and Dasannacharya B A 1991 *Physica* B **174** 112
[10] Godefroy G, Jannot B and Michel-Calendini F M 1991 *Phase Transitions* **33** 3 and references therein
[11] Darlington C N W and Cernik R J 1992 *J. Phys.: Condens. Matter* **4** 4387
[12] Darlington C N W and Cernik R J 1993 *J. Phys.: Condens. Matter* **5** 5963
[13] Sastry P U M, Sequeira A, Rajagopal H, Balakumar S, Ilangovan R and Ramansamy P 1996 *J. Phys.:
        Condens. Matter* **8** 2905
[14] Müller K A 1986 *Helv. Phys. Acta.* **59** 874
[15] Müller K A and Berlinger W 1986 *Phys. Rev.* B **34** 6130
[16] Low W and Shaltiel D 1958 *Phys. Rev. Lett.* **1** 51 and 286
[17] Hornig A W, Rempel R C and Weaver H E 1958 *Phys. Rev. Lett.* **1** 284
[18] Hornig A W, Rempel R C and Weaver H E 1959 *J. Phys. Chem. Solids* **10** 1
[19] Sakudo T 1963 *J. Phys. Soc. Japan* **18** 1626
[20] Sakudo T and Unoki H 1964 *J. Phys. Soc. Japan* **19** 2109
[21] Müller K A 1976 *Ferroelectrics* **13** 381
[22] Müller K A 1976 *Phys. Rev.* B **13** 3209
[23] Abragam A and Bleaney B 1970 *Electron Paramagnetic Resonance of Transition Ions* (Oxford: Clarendon)
[24] Rekha Rao, Roy A P, Dasannacharya B A, Balakumar S, Ilangovan R, Ramasamy P and Aggarwal M D
        1996 *Pramana J. Phys.* to be published